

An universal algorithm of calculating terms of atomic many-body perturbation theory

V. A. Dzuba

School of Physics, University of New South Wales, Sydney 2052, Australia

(Dated: October 26, 2018)

An algorithm, based on numerical description of the terms of many-body perturbation theory (Goldstone diagrams), is presented. The algorithm allows the use of the same piece of computer code to evaluate any particular diagram in any specific order of the perturbation theory or to calculate similar terms in other areas of the many-body theory, like e.g. terms in the coupled-cluster equations. The use of the algorithm is illustrated by calculating the second and third order correlation corrections to the removal energies of electrons from the ground state of sodium, copper and gallium and by calculating the hyperfine structure constants of sodium in the linearized single-double coupled cluster approximation.

PACS numbers: PACS: 31.15.Md,31.25.-v,31.25.Eb

I. INTRODUCTION

This paper discusses calculations of terms of the many-body theory which arise when a system of interacting particles is described with the use of a set of single-particle basis functions. We focus the discussion on the atomic many-body perturbation theory (MBPT). However, similar approach can be used in molecular, solid state, nuclear physics, etc. and is not limited to the perturbation theory. The approach relies on the numerical description of the structure of the terms (diagrams) and on an universal algorithm which calculates the terms according to their structure.

Many body perturbation theory (MBPT) is one of the most commonly used tools of performing calculations for many-electron systems. There is enormous number of examples of its successful application to atoms, molecules, etc. (see, e.g.[1, 2]). However, the use of MBPT has many technical difficulties. It is often insufficient to include only lowest-order terms to obtain desirable accuracy. But inclusion of higher orders leads to huge increase of the number of terms and, what is even more important, of the the number of different types of terms, or terms which have different structure. Following Goldstone diagram technique we will use graphic diagrams to show the structure of the terms. Common programming practice is to write a separate piece of computer code for each diagram. However, in higher orders the number of diagrams increases so dramatically that writing corresponding computer codes becomes a very difficult task.

There is certainly a need to automatize the use of the MBPT. This must include at least two stages: (1) generation of the diagrams, and (2) evaluation of the diagrams. These two tasks are closely related since diagrams are to be generated in a form which is then used for their calculation. Generation of diagrams was discussed in Ref. [3, 4, 5, 6, 7, 8]. We will not discuss it here but rather focus on the diagram evaluation assuming that the diagrams have unambiguous numerical description.

In the approach used by Derevianko *et al* [6, 7] diagrams are generated together with computer codes for their calculation. In present paper we present a different approach which is based on an universal algorithm in which diagram structure is presented by a set of parameters which are passed to a Fortran subroutine. This allows the use of a single piece of computer code to calculate any specific diagram.

We also don't discuss in this paper the task of calculation of the basis of single-electron states. The algorithm is independent of the basis apart from the fact that its current implementation assumes the use of basis functions which correspond to the spherically-symmetric case, i.e their dependence on angular coordinates is determined by spherical harmonics. The independence on the basis gives the users flexibility to use a basis which best fits their needs. We use the B-spline basis [9], an alternative choice is presented in Ref. [10]. In fact, any functions which constitute a complete set of states in a spherically-symmetric case can be used.

In this paper we first describe the idea behind the algorithm, the features of its current implementation, its efficiency and intended use. Then we describe the algorithm itself. Finally, we present two examples of its use. First is the many-body perturbation theory calculations of the second and third order correlation corrections to the removal energies for an external electron in the ground state of sodium, copper and gallium. Second is the calculation of the hyperfine structure of sodium in the linearized single-double coupled cluster approximation.

The technique developed in this work was recently used for the calculation of the relativistic energy shifts of frequencies of atomic transitions used in the search for variation of the fine structure constant in quasar absorption spectra [11]. The calculations were performed with the linearized couple-cluster single-double method complemented by the third-order MBPT. All third-order calculations were performed using the algorithm presented in this work.

II. GENERAL IDEA AND ITS IMPLEMENTATION

The algorithm does not represent an independent method of many-body calculations. It only represents a way of calculating terms (diagrams) in any many-body method such as MBPT, CC, etc. Current implementation of the algorithm has certain limitations which will be discussed below. However, the idea behind it is very general. It can be formulated in two statements:

1. The structure of a diagram can be described numerically.
2. Once an unambiguous numerical description of a diagram is given, a procedure can be build to evaluate the diagram according to its structure. This procedure can be a very general one, working for any diagram.

This approach can be used in any many-body theory which deals with a system of interacting particles and uses a set of single-particle basis functions. Current implementation has been developed for atomic calculations. It has features which are natural for atomic calculations and which impose some limitations on the use of the algorithm. In principle, most of these limitations can be eased or avoided with appropriate amendments to the algorithm. These features are:

- Spherical coordinates are used. It is assumed that there is a set of orthogonal and normalized single-electron basis states which are the eigenstates of the Dirac operator in the spherically-symmetric case. The basis orbitals have standard set of quantum numbers: $|i\rangle \equiv |njl m\rangle$, where n is principal quantum number, j is total momentum, l is angular momentum, m is projection of j . They may come from calculations in some spherically-symmetric potential, like Hartree-Fock potential of closed atomic shells, Coulomb nuclear potential, some parametric potential, etc. They can also be some artificial functions not directly relevant to any potential.

The angular dependence of the basis functions is determined by spherical spinors. This allows the use of standard angular momentum algebra to reduce integrals over angular variables to the $3j$ -symbols and to perform summation over projections m . This procedure, known as *angular reduction*, is done in the algorithm partly analytically and partly numerically. Integrals over angular variables are still expressed via the $3j$ -symbols analytically while summation over projections m is done numerically. Numerical approach to the summation over projections allows to perform it in a universal way, so that the procedure works for any diagram.

In principle, appropriate amendments to the numerical angular reduction part of the algorithm could extend it to a non-spherically-symmetric case.

- In present work we give detailed consideration only to diagrams with two free ends. These two free ends represent states of a valence electron and corresponding diagrams represent a correction to the removal energy of this electron due to correlations with the electrons in atomic core. With some minor modification the algorithm can also be used for diagrams with no free ends (e.g. correlation correction to the energy of atomic core), four ends (e.g. correlation correction to the Coulomb interaction between two valence atomic electrons), etc. In fact, we use the later version of the algorithm for solving of the single-double equations as is discussed in section V B.
- Present algorithm deals with radial integrals involving two or four basis functions. The former may represent e.g. matrix elements of an external field acting on an electron, while the later may represent matrix elements of the interaction between two electrons. This would cover most of the applications. However, there are cases when it is not enough. For example, triple excitation coefficients in the coupled-cluster method have properties of radial integrals involving six basis functions. Certain modification of the algorithm may include this case too.
- The task of calculating single and double-electron matrix elements is left to the user while only the rank of the operators is passed to the algorithm for numerical calculation of angular coefficients. This gives a lot of flexibility for the algorithm use. Not only the basis is chosen by the user but also interpretation of the single and double electron operators is left to the user. This allows to consider a wide range of problems without making any adjustments in the algorithm. For example, in most of cases the two-electron operator is likely to be an operator of the non-relativistic Coulomb interaction between electrons. But, depending on the problem, it can also be Breit relativistic correction to the inter-electron interaction, specific mass shift operator, double excitation coefficient in the coupled-cluster calculations, etc. There is even wider choice for a single-electron operator. This can be an interaction with external laser field, interaction of atomic electrons with electric and magnetic moments of the nucleus, etc. As a result, the same algorithm can be used for the MBPT calculations of atomic energy levels, fine and hyperfine structure, transition amplitudes, effects of parity non-conservation, single excitation coefficient, etc.

III. EFFICIENCY

The purpose of the algorithm discussed in this paper is to free researcher time from writing and testing computer codes whenever terms of a many-body theory need to be calculated. It provides a ready piece of code which can be used for any terms of any many-body method. In terms of computer resources needed in most of cases the use of the algorithm would be as efficient as writing new code. In some special cases when efficiency is important writing new code might still be a desirable alternative. A code written for specific diagram may take advantage of its structure to perform the calculations in the most efficient way. In contrast, the algorithm uses an uniform approach to all diagrams.

Computer time needed to calculate a diagram by the algorithm presented in this paper is given by

$$T = Ac^s v^p, \quad (1)$$

where A is a factor which depends on a computer and on the implementation of the algorithm, c is the number of occupied states, s is the number of summations over occupied states, v is the number of virtual states, and p is the number of summations over virtual states. It is assumed that all single-electron states with the same quantum numbers n, l, j but different projection m have the same radial function. Therefore, the factors c and v are much smaller than the total number of single-electron states. For example, the total number of electrons in the cesium core is 54, however the number of core states with different radial functions is 17, i.e. $c=17$ for Cs. The value of v depends on the basis. In present work we use the B-spline basis with 40 B-splines in each partial wave up to $l_{max} = 5$ which corresponds to $v = 440 - 17 = 423$.

Formula (1) suggests that the calculations become unwieldy in higher orders which have terms with large p . In our experience it is impractical to go beyond $p = 4$ unless a supercomputer is used. Terms with $p > 4$ first appear in the forth order of the MBPT. This is rather indicates inefficiency of the MBPT than inefficiency of the algorithm. When higher-orders need to be considered the best choice is to use some all-order technique like, e.g. coupled-cluster (CC) technique (see, e.g. [1, 12, 13]) or correlation potential method [14], etc. The CC technique includes terms with maximum number of summations over virtual states. Every iteration of the CC equations corresponds to the next order of the MBPT but takes exactly the same time. This means that the CC technique is much more efficient in higher orders than the MBPT. On the other hand the algorithm can be used to calculate terms in either of this methods, CC or MBPT alike.

A good example when the algorithm can be extremely useful comes from a comparison of the CC and MBPT techniques. The CC method misses certain contributions to the many-body wave function usually starting from the third order of the MBPT. Sometimes it is important to know the value of missed terms. The MBPT can be used for this purpose. The main obstacle on this way is a need to write huge amount of computer code to handle large number of diagrams in higher orders of the MBPT. In contrast, new new programming is needed when the algorithm is used.

We stress once more that the algorithms does not represent an independent method of calculations. It represents a way of evaluating terms in any many-body method. For example, it can be used to calculate terms in the CC equations or in MBPT, etc. In most cases it is sufficiently efficient, but in some cases it is not. Therefore, the general rule is the following. Give special consideration to the most computer demanding terms. These terms can be easily identified by large number of summations over virtual states and there are usually very few of them. Then use the algorithm for all other terms.

Note in the end that since the calculation of matrix elements is left to the user, the efficiency of the algorithm is partly in hands of the user as well. This cannot change formula (1) but can reduce the value of A in it. For example, with the sufficient computer memory, all single and double-electron integrals can be calculated in advance and stored in the computer memory. This would speed up the calculations enormously.

IV. ALGORITHM

A. Numerical representation of the diagrams

We use two levels of numerical representation of the diagrams. One is compact and easy to generate. It uniquely identifies a diagram but gives insufficient description for its actual calculation. A more detailed description must be created before the diagram can be calculated. This is also done automatically.

Following standard diagram technique we distinguish three types of electron states which are presented on a diagram by three different types on lines:

- *Core (occupied) state*. This is a state in the atomic core. It is shown by a line which starts and ends on a vertex and goes from right to left as shown by an arrow. It assumes summation over states of atomic core.

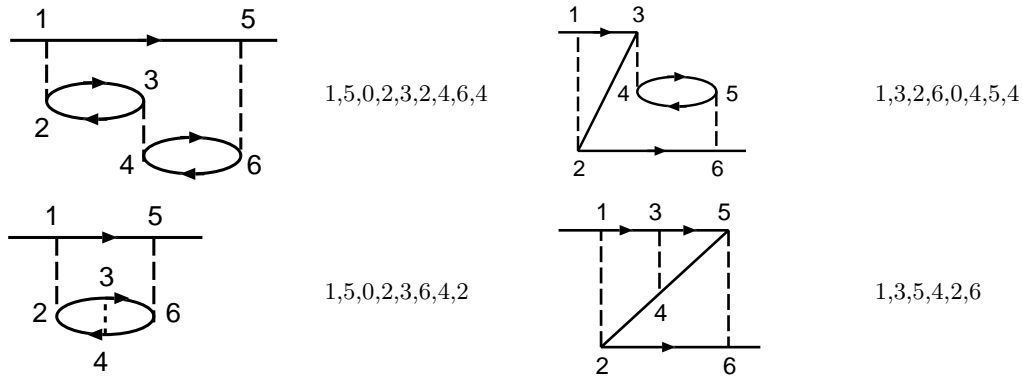


FIG. 1: Some third order Goldstone diagrams and their numerical representation

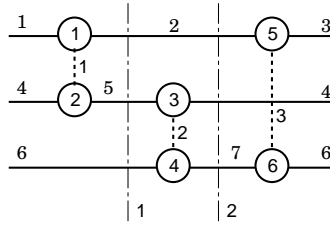


FIG. 2: Detailed numerical description of the first diagram from Fig. 1

- *Excited (virtual) state.* This is a state above atomic core. It is shown by a line which starts and ends on a vertex and goes from left to right as shown by an arrow. It assumes summation over all states above the core.
- *Valence state.* This is a state above atomic core for which matrix element represented by the diagram is calculated. It is shown by a line which starts or ends on a vertex and has a free end. It goes from left to right as all other states above the core. It assumes no summation.

Compact diagram representation is illustrated on Fig. 1. It is based on the following rules:

1. All vertexes are numerated from left to right. Every pair of vertexes corresponding to a two-electron operator have consequent numbers (1 and 2, 3 and 4, etc.).
2. The diagram description is created by listing the vertexes in order of their appearance while moving along a fermion line in the direction shown by an arrow.
3. Fermion line with valence states must be the first in the list. Zero index is used to separate it from the rest of the diagram.
4. Loops start and end with the same vertex number.

Fig. 2 illustrates detailed numerical description of the first diagram on Fig. 1. It is generated automatically. It presents the diagram in a form convenient for the calculations. Apart from vertexes it also numerate fermion lines

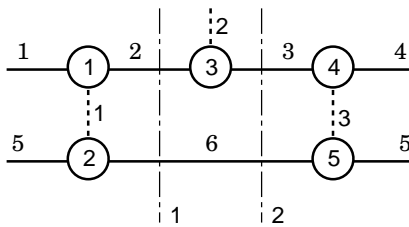


FIG. 3: Detailed numerical description of a diagram which contains interaction with external field (single-electron operator)

Vertex number	Left fermion line number	Boson line number	Right fermion line number
Diagram on Fig. 2			
1	1	1	2
2	4	1	5
3	5	2	4
4	6	2	7
5	2	3	3
6	7	3	6
Diagram on Fig. 3			
1	1	1	2
2	5	1	6
3	2	2	3
4	3	3	4
5	6	3	5

TABLE I: Vertexes description for diagrams on Fig 2 and Fig 3

Step	Result
1	1,5,0,2,3,2,4,6,4
2	1-f-5-0, 2-f-3-f-2, 4-f-6-f-4
3	1-e-5-0, 2-e-3-c-2, 4-e-6-c-4
4	v-1-e-5-v, 2-e-3-c-2, 4-e-6-c-4

TABLE II: Generation of the detailed description of the diagram A1. f is a fermion state (either core or excited), e is an excited state, c is a core state, v is a valence state.

(electron states) and boson lines (interactions). Fermion lines are shown on Fig. 2 as solid horizontal lines while boson lines are dotted vertical lines. Diagram cross-sections are also shown as dash-dotted lines. There are closed and open fermion lines. Closed lines start and end on vertexes. They assume summation over core or excited states. Open lines have one free end and correspond to valence states. They assume no summation. Note that lines 1 and 3 on Fig. 2 correspond to the same valence state. However they are given different indexes to indicate that there is no summation for these lines. On the other hand lines 4 and 6 are closed even though they are shown in two different pieces each. Table I shows that numerical description of each vertex consists of three whole numbers: left fermion line number, boson line number and right fermion line number. To complete the picture the type of every fermion line must be specified: core state, state above the core or valence state.

Automatic generation of detailed numerical description of a diagram starting from its compact representation follows the following rules:

- There is a fermion line between any pair of neighboring vertexes in the list (see Fig. 1).
- This line corresponds to a core state if second index is smaller or to a state above the core otherwise.
- There is a valence state before the very first index and before zero index or after the last index if no zero present.
- Boson lines are always between indexes 1 and 2, 3 and 4, etc.
- Vertexes, fermion and boson lines are numbered independently.

The process of generating a detailed description of diagram on Fig.2 is illustrated in Table II.

Fig. 3 shows detailed numerical description of a diagram which has an interaction with external field (e.g. electric dipole field of a photon). This is one of the so called *structure radiation* diagrams. Its numerical description is very similar to those on Fig. 2 with few minor differences: the order of the vertexes is not fixed and the type of each vertex must be specified (i.e. to which operator it corresponds). At the moment there is no automatic generation of this description and it has to be supplied manually.

B. Calculation of the diagrams

Diagrams differ from each other by number of summations over core and excited states, by indexes with enter every single- and double-electron matrix elements, by energy denominators and by angular coefficients. An universal

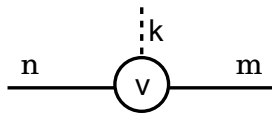


FIG. 4: Vertex corresponding to a single-electron operator.

algorithm must treat all these differences as parameters which affect what the program calculates but do not affect its structure. We will consider them in turn.

a. Main summation loop. The procedure set out in this paragraph is the result of discussions with J.S.M. Ginges.

Different diagrams usually have different number of summations over core and excited states. In a standard approach each summation is performed in a separate *do* loop. Since the number of *do* loops usually cannot be a parameter, here is the need for different code for each diagram. In present paper we use a single *do* loop for all summations:

$$S = \sum_{i=1}^{N_t} s_i. \quad (2)$$

Index of summation i runs over total number of terms N_t and all other indexes numerating single-electron basis states are calculated. The total number of terms for any diagram is given by

$$N_t = n_{cs}^{n_{cl}} n_{es}^{n_{el}}, \quad (3)$$

where n_{cs} is the number of core states, n_{cl} is the number of core lines in the diagram, n_{es} is the number of excited states (states above the core), and n_{el} is the number of lines in the diagram which represent states above the core. n_{el} does not include valence lines since they assume no summation.

Calculation of all indexes numerating single-electron states follow a simple recurrent algorithm. The indexes are ordered and the range of their change is determined. For every new term in the summation first index is incremented by one. When it exceeds its maximum value, it goes back to its minimum value and next index is incremented by one, etc.

b. Energy denominators. Total energy denominator of a diagram is calculated as a product of the energy denominators corresponding to particular diagram cross-sections

$$\Delta_{total} = \prod_{i=1}^{N_{cs}} \Delta_i. \quad (4)$$

Here N_{cs} is the number of cross-sections for the diagram. A cross-section is a vertical line which crosses fermion lines between diagram vertexes (see Figs. 2 and 3). Recurrent formulas are used to calculate Δ_i . First

$$\Delta_0 = 0. \quad (5)$$

Then

$$\Delta_i = \Delta_{i-1} + \epsilon_n - \epsilon_m + \omega, \quad (6)$$

for a single-electron operator (see Fig. 4) or

$$\Delta_i = \Delta_{i-1} + \epsilon_n + \epsilon_l - \epsilon_m - \epsilon_j \quad (7)$$

(see Fig. 5). Here ϵ_i is the energy of the single-electron basis state number i , ω is the frequency of external monochromatic field ($\omega = 0$ for static fields).

c. Calculation of single- and double-electron matrix elements Every term in (2) is a product of single- and double-electron matrix elements and an angular coefficient. The later will be considered in next paragraph. As for the product of the single- and double-electron matrix elements its calculation follows the same pattern as the calculation of the energy denominators. A transition to every next cross-section of a diagram is caused by a single-electron matrix element or by a double-electron matrix element (as on Figs. 4,5). All indexes numerating single-electron basis states are known on this stage. Therefore, they just passed to the sections of the program which is assumed to be supplied by the user.

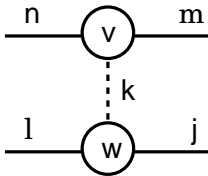


FIG. 5: Vertex corresponding to a double-electron operator.

Leaving to the user calculation of the single- and double electron matrix elements gives a lot of flexibility to the algorithm.

First, it allows different interpretation of the operators at user discretion. For example, in most of cases the double-electron matrix element would probably be the matrix element of non-relativistic Coulomb interaction between electrons. However, it can also be a matrix element of Breit operator (relativistic correction to the Coulomb interaction[15, 16]), or specific mass shift operator[17], etc.

There is even larger choice for the single-electron operator. This can be, e.g. electron interaction with nuclear magnetic dipole or nuclear electric quadrupole moments for calculation of the hyperfine structure of atomic levels, it can be interaction of atomic electrons with electric or magnetic laser field for the calculation of transition amplitudes, etc.

The single and double-electron matrix elements can also be interpreted as single and double-excitation coefficients in the coupled-cluster expansion of the many-electron wave function[12]. Therefore, the algorithm can be used for solving the single-double coupled-cluster equations.

Second, the user's interpretation of matrix elements allows the use of different basis states. For example, B-spline basis is used in present work[9]. But it can be a basis of real Hartree-Fock states, or states calculated in a parametric potential, Coulomb basis, etc.

Finally, it allows to choose an efficient way of calculating matrix elements. This is especially important for the double-electron matrix elements, since their calculation usually takes most of the computer time in the MBPT calculations. In the example presented in section V A below we calculate Coulomb integrals via Coulomb Y -functions as it was done in our other works[11, 18]. The Y -functions are calculated in advance and stored on disk. The most obvious alternatives to this are to calculate Coulomb integrals from single-electron wave functions every time they are needed, or to calculate them in advance and store on a disk or in computer memory.

d. Numerical angular reduction. Calculation of the angular coefficient consists of two parts. First, summation over projections and second, calculation of the projection independent part.

Summation over projections is performed numerically using the same ideas as for the whole diagram. Summation is done in a single *do* loop which runs over total number of terms which is given by

$$N_t = \prod_{i=1}^{n_{fl}} (2j_i + 1). \quad (8)$$

Here $n_{fl} = n_{cl} + n_{el}$ is the total number of fermion lines in the diagram, not counting the valence lines, j_i is the total momentum of the single-electron state number i . Note that the boson lines don't need to be included into the counting of the number of terms. This is because corresponding projection is fixed by the condition $-m_n + q + m_m = 0$, where m_n and m_m are the projections of j_n and j_m . Valence lines also don't contribute to the number of terms (8) because they involve no summation.

Each vertex (see, e.g. Fig.4) is associated with the $3jm$ -symbol

$$(-1)^{j_n - m_n} \begin{pmatrix} j_n & k & j_m \\ -m_n & q & m_m \end{pmatrix}. \quad (9)$$

Here k is the multipolarity of Coulomb interaction or a rank of single-electron operator. Every term in the summation over projections is calculated as a product of $3jm$ -symbols corresponding to all vertexes of the diagram.

Projection-independent part of the angular coefficient corresponding to Coulomb interaction is calculated as a product of terms

$$(-1)^{j_m + j_j + 1} \sqrt{(2j_n + 1)(2j_m + 1)(2j_l + 1)(2j_j + 1)} \begin{pmatrix} j_n & k & j_m \\ -\frac{1}{2} & 0 & \frac{1}{2} \end{pmatrix} \begin{pmatrix} j_n & k & j_m \\ -\frac{1}{2} & 0 & \frac{1}{2} \end{pmatrix} \quad (10)$$

for every pair of Coulomb vertexes (as on Fig.5).

Calculations of the projection-independent part of a single-electron operator is left to the user.

V. EXAMPLES

A. Correlation corrections to the ground-state energies of sodium, copper and gallium

In this section we present the calculation of the energies of the ground states of sodium, copper and gallium using relativistic Hartree-Fock method (RHF) and second and third-order of the many-body perturbation theory in residual Coulomb interaction. All second and third order diagrams are calculated using the technique described above.

Sodium, copper and gallium represent three different and most common types of electron structure for atoms with one external electron above closed shells. MBPT calculations for them is a good illustration on how the MBPT works for different atomic systems and how it can be used to significantly improve the accuracy of the calculations. Calculations for sodium in second and third-order were considered before in Ref.[19]. This gives us an opportunity to compare the results. To the best of our knowledge other two atoms were not considered before to the third order of the MBPT.

We use the V^{N-1} approximation, which is the standard approach for atoms with one valence electron. Initial Hartree-Fock procedure is performed for a closed-shell ion, with the valence electron removed. Then, the states of the valence electron are calculated in the field of frozen core. We use the B-spline technique[9] to construct a full set of single-electron orbitals. We use 40 B-splines of order $k = 9$ in each partial wave up to maximum angular momentum $l_{max} = 5$. Single-electron basis functions are calculated as linear combination of B-splines in a cavity of radius $R_{max} = 40a_B$ which are eigenstates of the relativistic Hartree-Fock Hamiltonian.

Calculations of the second-order correlation corrections are relatively simple and were considered many times before (see, e.g.[19, 21, 22]). We will not discuss them here focusing rather on the third-order corrections. Third-order correlation corrections for the energies of the single-valence electron atoms were discussed before in Refs.[20, 23]. The total number of the third order diagrams is 76. This can be reduced to 52 if symmetry conditions are used. This can be further reduced to 12 if direct and exchange terms are grouped together. We follow Ref.[20] to name these 12 terms by letters from A to L. The results of calculations are presented in Table III separately for most of the 52 diagrams.

All diagrams are calculated with the same piece of code using numerical description of the diagrams as presented in the second column of the table. Some diagrams are grouped together with their exchange companions. This is indicated in the *comment* column of the table. For example, diagram A2 is an exchange companion of diagram A1. They were calculated together and only the sum is presented in the table. This is indicated as the A1+A2 comment in the table. Diagrams C,D,G,H,K and L have complex conjugated companions with exactly the same value. This can be taken into account by multiplying the diagrams by the factor of 2 as indicated in the table.

There is strong cancellation between contributions from different diagrams, the strongest is for diagrams I and J (see also Refs.[20, 23]). The final answer for the total third-order correction is much smaller than the largest contributions. However, the final answer is stable and not very much sensitive to numerical uncertainty. This is because all diagrams are calculated in a very similar way which leads to cancellation of numerical error.

Table IV summarize the results of the calculations for the ground-state energies of Na, Cu and Ga in the RHF approximation and with inclusion of the second-order (E2) and third-order (E3) correlation corrections. For gallium we include both components of the fine structure doublet. The sum of all contributions (RHF+E2+E3) is compared with experiment.

The analysis of the correlations show some differences as well as similarities between the elements. The total value of the correlation correction which is the difference between the RHF and experimental values (we neglect Breit and QED corrections here) is 3.6% for Na, 15% for Cu and 11% for Ga. The correlations are strongly dominated by the second order as it is well known from a number of calculations (see, e.g.[20, 21, 23]). However, the third-order correlation correction is not small and its inclusion leads to further significant improvement of the results for all three atoms. This is especially prominent for the case of copper where the third-order correction is only four times smaller than the second-order correction and constitutes about 3% of the experimental value. However, the final result for copper is within 1% of the experiment.

Fine structure interval of the $4p$ ground state of gallium is also significantly improved when second and third-order correlation corrections are included (see Table IV).

The results for sodium presented in this section are in good agreement with previous calculations[19].

B. Calculation of the hyperfine structure of sodium in the SD approximation

It is known that many properties of light alkaline atoms can be described to high precision within the linearized single-double coupled cluster approximation (SD) (see, e.g. Ref. [25]). In this approximation the many-electron wave function of an atom is written as an expansion over single and double excitations from the reference Hartree-Fock wave

Diagram as in Ref. [20]	Its numerical representation	$\delta E^{(3)}$				Comment
		Na, 3s	Cu, 4s	Ga, 4p _{1/2}	Ga, 4p _{3/2}	
A1	1,5,0,2,3,2,4,6,4					
A2	1,3,2,6,0,4,5,4	180	2024	1851	1815	(A1+A2)
A3	1,5,0,2,3,6,4,2	-352	-2639	-3310	-3260	
A4	1,3,5,4,2,6,0	25	326	692	679	
A5	1,5,4,6,0,2,3,2	-11	8	-234	-229	
A6	1,3,2,5,4,6,0	7	101	191	186	
A7	1,5,3,2,4,6,0					
A8	1,3,5,0,2,6,4,2	-217	-1970	-2369	-2320	(A7+A8)
B1	5,1,0,2,3,2,4,6,4					
B2	5,1,4,2,0,3,6,3	-59	-196	-681	-659	(B1+B2)
B3	5,1,0,2,3,6,4,2	83	290	1156	1119	
B4	5,1,3,6,4,2,0	-32	-126	-478	-469	
B5	5,3,6,2,0,1,4,1	25	67	329	320	
B6	5,3,6,1,4,2,0	-9	-27	-127	-123	
B7	5,3,1,4,6,2,0					
B8	5,3,1,0,2,4,6,2	48	180	580	556	(B7+B8)
C1	3,5,0,1,4,1,2,6,2	251	2631	1523	1489	2×C1
C2	3,5,0,1,4,2,6,1	-55	-450	-489	-480	2×C2
C3	3,1,4,5,0,2,6,2					
C4	3,1,5,2,4,6,0	-33	-50	-267	-259	2×(C3+C4)
C5	3,5,2,6,0,1,4,1	-15	-50	-219	-214	2×C5
C6	3,5,1,4,2,6,0	7	48	90	88	2×C6
C7	3,1,4,5,2,6,0					
C8	3,1,5,0,2,4,6,2	-33	-133	-174	-170	2×(C7+C8)
D1	5,3,0,1,4,1,2,6,2	-137	-560	-807	-784	2×D1
D2	5,3,0,1,4,2,6,1	34	115	245	238	2×D2
D3	5,3,1,4,0,2,6,2					
D4	5,3,1,6,2,4,0	97	378	569	544	2×(D3+D4)
D5	5,1,6,3,0,2,4,2	83	105	296	290	2×D5
D6	5,1,3,2,6,4,0	-12	-37	-111	-108	2×D6
D7	5,1,6,3,2,4,0					
D8	5,1,3,0,2,6,4,2	65	259	534	510	2×(D7+D8)
E	1,3,5,0,2,4,6,2	237	1913	3098	3045	(E1+E2)
F	5,3,1,0,2,6,4,2	-54	-220	-606	-582	(F1+F2)
G	5,1,3,0,2,4,6,2	-75	-349	-730	-700	2×(G1+G2)
H	3,1,5,0,2,6,4,2	26	54	28	27	2×(H1+H2)
I1	3,0,1,5,4,1,2,6,2					
I2	3,1,5,4,0,2,6,2	-4692	-22898	-19732	-19486	(I1+I2)
I3	3,0,1,6,2,5,4,1					
I4	3,1,5,2,6,4,0	1509	5361	5902	5833	(I3+I4)
J1	3,0,1,4,5,1,2,6,2	4603	21668	19018	18807	(J1+J2)
J3	3,0,1,4,5,2,6,1	-1480	-5072	-5644	-5584	(J3+J4)
K1	5,0,1,6,3,1,2,4,2	-290	-5272	-895	-862	2×(K1+J2)
K3	5,3,1,6,0,2,4,2	-55	-1666	-275	-264	2×(K3+J4)
L1	5,0,1,3,6,1,2,4,2	267	3181	1046	1009	2×(L1+J2)
L3	5,1,3,6,0,2,4,2	28	953	230	230	2×(L3+J4)
Total		-82	-2054	826	830	

TABLE III: Third order contributions to the ground state energies of sodium, copper and gallium (cm⁻¹).

	Sodium		Copper		Gallium	
	3s	4s	4p _{1/2}	4p _{3/2}	4p _{1/2}	4p _{3/2}
RHF	-39951	-52302	-43033	-42294		
E2	-1277	-7607	-6404	-6280		
E3	-82	-2054	826	830		
Total	-41310	-61963	-48611	-47744		
Experiment[24]	-41450	-62317	-48380	-47554		

TABLE IV: Ground state energies of sodium, copper and gallium (cm⁻¹) in RHF approximation, second-order correlation corrections(E2) and third-order correlation correction(E3); comparison with experiment.

functions. Expansion coefficients ρ satisfy the set of self-consistent equations. The SD equations for the excitations from the atomic core have the form

$$\begin{aligned}
(\epsilon_a - \epsilon_m)\rho_{ma} &= \sum_{bn} \tilde{g}_{mban}\rho_{nb} + \sum_{bnr} g_{mbnr}\tilde{\rho}_{nrab} - \sum_{bcn} g_{bcn}\tilde{\rho}_{mnbc}, \\
(\epsilon_a + \epsilon_b - \epsilon_m - \epsilon_n)\rho_{mnab} &= g_{mnab} + \sum_{cd} g_{cdab}\rho_{mncd} + \sum_{rs} g_{mnr s}\rho_{rsab} \\
&+ [\sum_r g_{mnr b}\rho_{ra} - \sum_c g_{cnab}\rho_{mc} + \sum_{rc} \tilde{g}_{cnrb}\tilde{\rho}_{mrac}] + \left[\begin{array}{c} a \leftrightarrow b \\ m \leftrightarrow n \end{array} \right].
\end{aligned} \tag{11}$$

Here parameters g are Coulomb integrals

$$g_{mnab} = \int \int \psi_m^\dagger(r_1)\psi_n^\dagger(r_2)e^2/r_{12}\psi_a(r_1)\psi_b(r_2)d\mathbf{r}_1d\mathbf{r}_2,$$

parameters ϵ are the single-electron Hartree-Fock energies. Coefficients ρ are to be found by solving the equations iteratively starting from

$$\rho_{mnij} = \frac{g_{mnij}}{\epsilon_i + \epsilon_j - \epsilon_m - \epsilon_n}.$$

Indexes a, b, c numerate states in atomic core, indexes m, n, r, s numerate states above the core, indexes i, j numerate any states.

The SD equations for a particular valence state v can be obtained from (12) by replacing index a by v and replacing ϵ_a by $\epsilon_v + \delta\epsilon_v$ where

$$\delta\epsilon_v = \sum_{mab} g_{abvm}\tilde{\rho}_{mvab} + \sum_{mnb} g_{vbm n}\tilde{\rho}_{mnvb}$$

is a correction to the energy of the valence electron. The SD equations are solved iteratively first for the core and than for as many valence states v as needed. The hyperfine structure (hfs) constants are found as an expectation values of the hfs operator over the SD wave functions.

Here we would like to demonstrate that the terms in the SD equations (12) as well as the expressions for the matrix elements (see below) can have numerical representation which opens a way for their evaluation using the algorithm described above. Before doing so let's note that computation time for solving the SD equations is strongly dominated by single term containing double summation over virtual states

$$\sum_{rs} g_{mnr s}\rho_{rsab}. \tag{12}$$

Therefore, it can be coded separately, using the most efficient way of its evaluation. All other terms can be treated by the universal algorithm. This is very general approach to the most efficient use of the algorithm: give special attention to the most computationally demanding terms (there are usually very few of them), use the algorithm for everything else.

Note also, that in contrast to the standard MBPT expressions the terms in the SD equations (12) have no energy denominators. Therefore, the algorithm should be modified to remove calculations of the energy denominators. This makes it even simpler.

We use whole numbers as specified in Table V for the numerical description of the terms in (12). Each of the values (ρ or g) are described as a sequence of three (for ρ_{ij}) or five (for ρ_{ijkl} or g_{ijkl}) whole numbers. First of these numbers indicate the type of the value (ρ , $\tilde{\rho}$, g or \tilde{g}), other numbers are the indexes. Negative numbers are used for occupied states and positive numbers are used for virtual or valence states. Summation is assumed over repeated indexes. Zero is used as a delimiter. Numerical representation of the SD terms (apart from the (12) is given in Table VI. This representation can be easily translated into a detailed diagram description discussed in section IV A.

Once the SD equations are solved for the core and for the valence states of interest, the hfs constants for these valence states can be calculated as expectation values of the hfs operator over the SD vale function. Corresponding expressions can be found in Ref. [25] and Table VII. We also present in the Table the numerical representation of these terms. It is very similar to the case of the SD terms with one small difference. Now we have to distinguish between single excitation coefficients ρ_{ij} and single-electron matrix elements of the hfs operator. We use indexes 1 and 2 for this purpose.

The results presented in the Table are in good agreement with the calculations of Ref. [26] and with experiment.

Notation	Its numerical representation	Comment
ρ	1	ρ_{ij} or ρ_{ijkl}
$\tilde{\rho}$	2	$\tilde{\rho}_{ijkl} = \rho_{ijkl} - \rho_{ijlk}$
g	3	Coulomb integral g_{ijkl}
\tilde{g}	4	$\tilde{g}_{ijkl} = g_{ijkl} - g_{ijlk}$
a, b, \dots	-1, -2, ...	Occupied (core) states
m, n, \dots	1, 2, ...	Virtual or valence states

TABLE V: Numerical representation of the parameters and variables of the SD equations.

Term	Its numerical representation
$g_{cdab}\rho_{mncd}$	3,-3,-4,-1,-2,0,1,1,2,-3,-4
$g_{mnr b}\rho_{ra}$	3,1,2,3,-2,0,1,3,-1
$g_{cnab}\rho_{mc}$	3,-3,2,-1,-2,0,1,1,-3
$\tilde{g}_{cnrb}\tilde{\rho}_{mrac}$	4,-3,2,3,-2,0,2,1,3,-1,-3

TABLE VI: Numerical representation of the terms of the SD equations

VI. CONCLUSIONS

We present an universal algorithm of calculating terms of the many-body perturbation theory. The algorithm assumes the basis of spherically symmetric relativistic single-electron states with the n, j, l, m quantum numbers. Apart from this and available computer power the algorithm is practically free from any limitations. It can be used to calculate any diagram of any order of MBPT with any set of single and double electron operators.

The algorithm presents a way to go to higher-orders of MBPT when sufficient computer power is available. It can also be used for solving single-double coupled-cluster equations or for any other calculations involving terms similar to those of the MBPT.

Calculations of the second and third order correlation corrections to the removal energies of electrons from the

SD terms as in Ref. [25]	Their numerical representation	$3s_{1/2}$	$3p_{1/2}$
z_{vw}		623.75	63.43
a $z_{am}\tilde{\rho}_{wmva} + c.c.$	2,-1,1,0,2,2,1,3,-1	122.43	15.34
b $-z_{av}\rho_{wa} + c.c.$	2,-1,1,0,1,2,-1	16.48	2.45
c $z_{wm}\rho_{mv} + c.c.$	2,2,1,0,1,1,3	104.94	10.17
d $\rho_{mv}z_{mn}\rho_{nv}$	1,3,1,0,2,1,2,0,1,2,4	4.41	0.43
e $\rho_{vb}z_{ab}\rho_{wa}$	1,1,-1,0,2,-1,-2,0,1,-2,2	0.11	0.03
f $-z_{av}\rho_{mw}\rho_{ma} + c.c.$	2,2,-1,0,1,-1,1,0,1,1,3	0.78	0.10
g $-z_{mv}\rho_{ma}\rho_{wa} + c.c.$	2,2,1,0,1,1,-1,0,1,-1,3	0.01	0.01
h $\rho_{nw}\tilde{\rho}_{nmva}z_{am} + c.c.$	2,3,-1,1,2,0,1,1,4,0,2,2,-1	8.07	0.86
i $\rho_{ma}z_{mn}\tilde{\rho}_{wnva} + c.c.$	2,3,-1,4,1,0,2,1,2,0,1,2,-1	0.06	0.05
j $-\rho_{mb}\tilde{\rho}_{wmva}z_{ab} + c.c.$	2,2,-1,3,1,0,1,1,-2,0,2,-2,-1	0.27	0.09
k $\rho_{vb}\tilde{\rho}_{wmab}z_{am} + c.c.$	1,2,-2,0,2,-1,-2,3,1,0,2,1,-1	0.94	0.11
l $-z_{av}\rho_{mb}\tilde{\rho}_{wmab} + c.c.$	2,2,-1,0,1,1,-2,0,2,-1,-2,3,1	-0.41	-0.07
m $-z_{mv}\rho_{na}\tilde{\rho}_{nmwa} + c.c.$	2,3,1,0,2,1,2,-1,4,0,1,-1,2	-1.35	-0.10
n $z_{ab}\rho_{mnb}\tilde{\rho}_{nmva}$	2,-1,-2,0,2,3,-2,1,2,0,1,1,2,4,-1	0.96	0.30
o $\tilde{\rho}_{vmbc}z_{ab}\tilde{\rho}_{wmac}$	2,2,1,-1,-3,0,2,-1,-2,0,2,-2,-3,3,1	4.12	0.65
p $\tilde{\rho}_{rmwa}z_{mn}\tilde{\rho}_{rnva}$	2,4,-1,3,1,0,2,1,2,0,2,3,2,5,-1	10.68	0.81
q $z_{mn}\rho_{vmab}\tilde{\rho}_{wnba}$	2,1,2,0,1,3,2,-1,-2,0,2,-1,-2,4,1	1.61	0.08
r $-\tilde{\rho}_{vnwb}z_{am}\tilde{\rho}_{nmab} + c.c.$	2,3,1,4,-2,0,2,-2,-1,2,1,0,2,2,-1	3.47	0.44
s $z_{av}\rho_{mnb}\tilde{\rho}_{nmab} + c.c.$	2,3,-1,0,2,-1,-2,1,2,0,1,1,2,4,-2	-7.19	-0.75
t $-z_{mv}\rho_{nab}\tilde{\rho}_{wnba} + c.c.$	2,3,1,0,1,1,2,-1,-2,0,2,-1,-2,4,2	-7.88	-1.02
Sum a to t		262.51	29.97
Normalization		1.004	1.001
Final		882.85	93.26
Experiment[27, 28]		885.8	94.44(13)

TABLE VII: Hyperfine structure constants for ^{23}Na (MHz) in the SD approximation.

ground-states of sodium, copper and gallium as well as the hyperfine structure constants of sodium in the SD approximation demonstrated the use of the technique. The total number of terms handled by the algorithm in these calculations is about one hundred and the calculations would be very difficult without it.

Acknowledgments

The author is grateful to J.S.M. Ginges, S. Blundell, and W. R. Johnson for useful discussions. The work is partly supported by the Australian Research Council.

-
- [1] I. Lindgren and J. Morris, *Atomic Many-Body Theory*, (Springer, Berlin, 1982).
 - [2] S. Wilson, *Comp. Phys. Rep.* **2** (1985) 391-480.
 - [3] J. Paldus and H. C. Wong, *Comput. Phys. Comm.* **6**, (1973) 1; *Comput. Phys. Comm.* **6**, (1973) 9.
 - [4] Z. Csepes and J. Pipek, *J. Comput. Phys.* **77**, 1 (1988).
 - [5] J. Lyons, D. Moncrieff and S. Wilson, *Comp. Phys. Commun.* **84** (1994) 91-101.
 - [6] A. Derevianko and E. D. Emmons, *Phys. Rev. A* **66**, (2002) 012503.
 - [7] C. C. Cannon and A. Derevianko, *Phys. Rev. A* **66**, (2002) 012503.
 - [8] R. J. Mathar, *Int. J. Quant. Chem.* **107**, (2007) 1975.
 - [9] W. R. Johnson and J. Sapirstein, *Phys. Rev. Lett.* **57**, (1986) 1126; W. R. Johnson, M. Idrees, and J. Sapirstein, *Phys. Rev. A* **35**, (1987) 3218; W. R. Johnson, S. A. Blundell and J. Sapirstein, *Phys. Rev. A* **37**, (1988) 307.
 - [10] K. Bely, A. Derevianko, *Comp. Phys. Comm.* **179** (2008) 310.
 - [11] V. A. Dzuba, and W. R. Johnson, *Phys. Rev. A* **76**, (2007) 062510.
 - [12] S.A. Blundell, W.R. Johnson, Z.W. Liu, and J. Sapirstein, *Phys. Rev. A* **40**, (1989) 2233. S.A. Blundell, W.R. Johnson, and J. Sapirstein, *Phys. Rev. A* **43**, (1991) 3407.
 - [13] R. Pal, M. S. Safronova, W. R. Johnson, A. Derevianko, and S. Porsev, *Phys. Rev. A* **75**, (2007) 042515.
 - [14] V. A. Dzuba, V. V. Flambaum, and O. P. Sushkov, *Phys. Lett. A.*, **140**, (1989) 493.
 - [15] G. Breit, *Phys. Rev.* **34**, (1929) 553; **36**, (1930) 383; **39**, (1932) 616.
 - [16] V. A. Dzuba, V. V. Flambaum, M. S. Safronova, *Phys. Rev. A*, **73** (2006) 022112.
 - [17] J. C. Berengut, V. A. Dzuba, V. V. Flambaum, *Phys. Rev. A*, **68**, (2003) 022502.
 - [18] V.A. Dzuba and V.V. Flambaum, *Phys. Rev. A*. **75**, (2007) 052504.
 - [19] M. S. Safronova, A. Derevianko, and W. R. Johnson *Phys. Rev. A* **58**, (1998) 1016.
 - [20] S. A. Blundell, W. R. Johnson, and S. Sapirstein, *Phys. Rev. A* **42**, (1990) 3751.
 - [21] V. A. Dzuba, V. V. Flambaum, O. P. Sushkov, *J. Phys. B: At. Mol. Phys.*, **16**, (1983) 715-722.
 - [22] W.R. Johnson, M. Idrees, and J. Sapirstein, *Phys. Rev. A* **35**, (1987) 3218.
 - [23] S. A. Blundell, W. R. Johnson, and S. Sapirstein, *Phys. Rev. A* **38**, (1988) 4961.
 - [24] C. E. Moore, *Atomic Energy Levels*, Natl. Bur. Stand. (US), Circ. No. 467 (Washington). vol. **1,2** (1958).
 - [25] S. A. Blundell, W. R. Johnson, Z. W. Liu, and J. Sapirstein, *Phys. Rev. A*. **40**, (1989) 2233.
 - [26] M. S. Safronova, W. R. Johnson, and A. Derevianko, *Phys. Rev. A* **60**, (1999) 4476.
 - [27] W. Happer in *Atomic Physics 4*, eds. G. zu Putlitz, E. W. Weber, and A. Winnacker, (Plenum Press, New York, 1974), pp. 651-682.
 - [28] W. A. Wijngaarden and J. Li, *Z. Phys. D* **32**, (1994) 67.